

## EXPERIMENTAL INVESTIGATION OF THREE DIMENSIONAL MAGNETIC RECONNECTION BY USE OF TWO COLLIDING SPHEROMAKS

Y. Ono<sup>1</sup>, T. Akao<sup>1</sup>, A. Morita<sup>1</sup>, M. Katsurai<sup>1</sup>, and M. Yamada<sup>2</sup>

<sup>1</sup> *Department of Electrical Engineering, University of Tokyo,  
7-3-1 Hongo, Bunkyo-ku, Tokyo 113, Japan*

<sup>2</sup> *Princeton Plasma Physics Laboratory, Princeton, New Jersey 08543, U.S.A*

### Abstract

Three-dimensional (3-D) effects of magnetic reconnection dynamics have been investigated experimentally by use of axially colliding plasma toroids with parallel and antiparallel toroidal magnetic fields. Reconnection speed is observed to increase as the reconnection angle between the merging field lines is increased from  $\sim 20^\circ$  to  $180^\circ$ . This difference is attributed to the compressibility of the neutral current sheet that tends to increase with increasing the magnetic field component parallel to the reconnection (X) line.

### 1. Introduction

New 3-D dynamics of magnetic reconnection have been investigated experimentally by use of axially colliding plasma toroids in the TS-3 device[1-3]. Our experiment has made an unique approach to reconnection dynamics: extension of 2-D local geometry of reconnection to 3-D global one by use of a new merging method. To date, most of reconnection models have utilized the 2-D geometry as in Fig. 1(a), where only two components of magnetic field parallel to the same plane are taken into account. As shown in Figs. 1(b),(b'),(c) and (c'), we include the third component of magnetic field that is normal to the plane i.e., parallel to the X-line, introducing a reconnection angle  $\theta$  between reconnecting field lines. Experimentally, two toroidal shape plasmas: spheromaks with parallel toroidal currents  $I_t$  are collided to merge in the axial direction, as shown in Fig. 2(a). The reconnection angle  $\theta$  is varied by changing (1) the polarities of their internal toroidal fields  $B_t$ , (2) the magnitude of externally applied toroidal field  $B_{t,ext}$ . In the method (1), the cohelicity merging with parallel  $B_t$  realizes  $\theta \sim 90^\circ$  (Fig. 1(b)) and the counterhelicity merging with antiparallel  $B_t$  does  $\theta \sim 180^\circ$  (Fig. 1(b')). The method (2) enables us to control  $\theta$  of these merging toroids continuously from  $0^\circ$  to  $180^\circ$ .

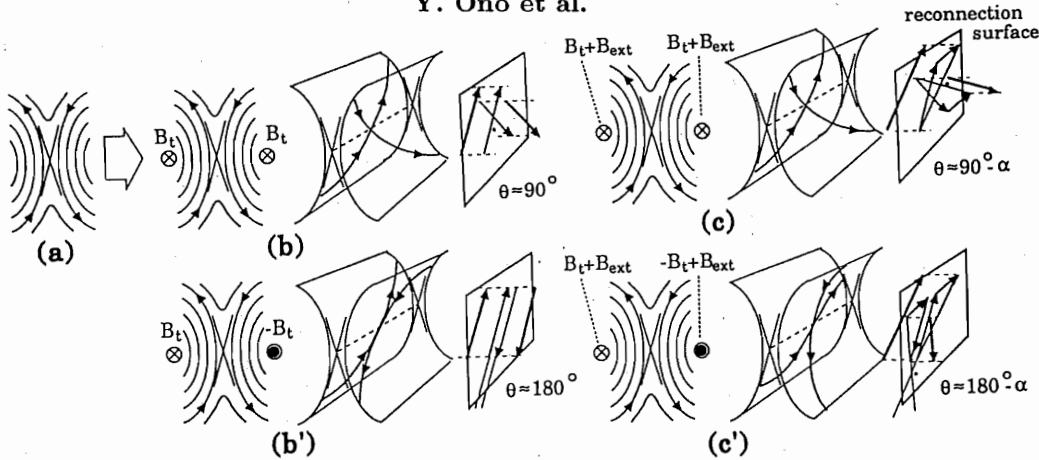


Fig. 1. 2-D local model of magnetic reconnection (a) and extended 3-D global models including the third component of magnetic field (b)-(c'). (b) and (b') show the cohesivity merging with  $\theta \sim 90^\circ$  and the counterhelicity merging with  $\theta \sim 180^\circ$ , respectively. The  $\theta$  value is also varied continuously from  $0^\circ$  to  $180^\circ$  by applying the external toroidal field to the cohesivity (c) and counterhelicity merging toroids (c').

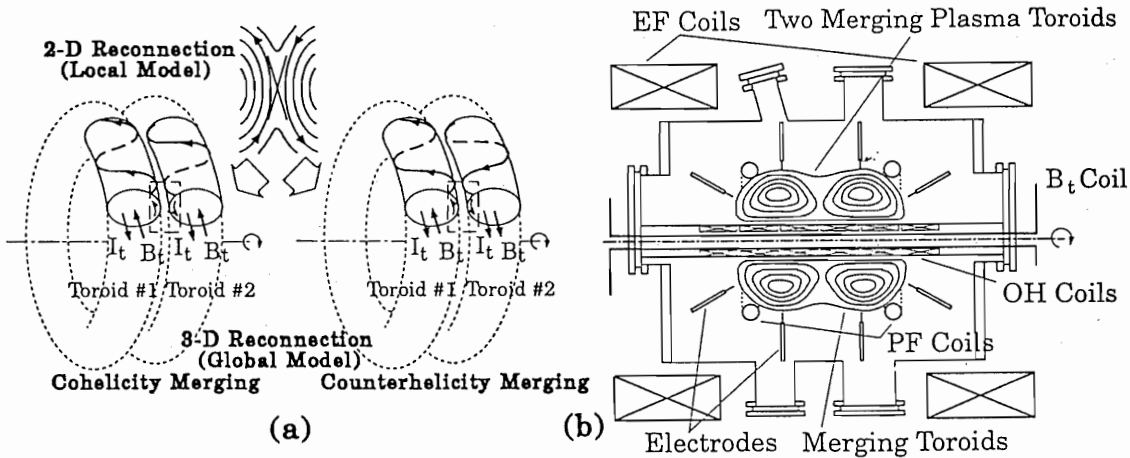


Fig. 2. Realization of 3-D reconnection by use of cohesivity and counterhelicity mergings (a), and  $Z$ - $\theta$ -pinch type setup of the TS-3 merging device (b)

## 2. Experimental Setup

Our TS-3 device can provide both  $Z$ - $\theta$ -pinch type (Fig. 2(a)) and gun type setups for this merging experiment. In the former setup, its cylindrical vacuum vessel has two internal poloidal field (PF) coils to produce the poloidal fluxes of the two initial spheromaks and also two sets of eight pairs of electrodes whose  $Z$ -discharges produce their toroidal fluxes with arbitrary polarity. The combination of the  $B_t$  polarities determines the type of merging with cohesivity or counterhelicity. The two spheromaks with major radii 15cm-20cm have typical temperature (initially  $T_e \sim T_i$ ) 10-20eV and electron density  $5\text{-}10 \times 10^{19} \text{m}^{-3}$ . An  $8 \times 7$  magnetic probe array is located on the  $r$ - $z$  plane to measure the 2-D profile of axial magnetic field  $B_z$ . Based on these probe data, 2-D contours of poloidal flux function  $\Psi(r, z) = \int_0^r 2\pi r' B_z dr'$  and those of toroidal current density  $j_t(r, z)$  are computed in a single discharge. The line averaged electron density  $\bar{n}_e$  and ion temperature  $\bar{T}_i$  are measured by a  $\text{CO}_2$  laser interferometer and by a visible light spectroscopy (doppler broadening), respectively.

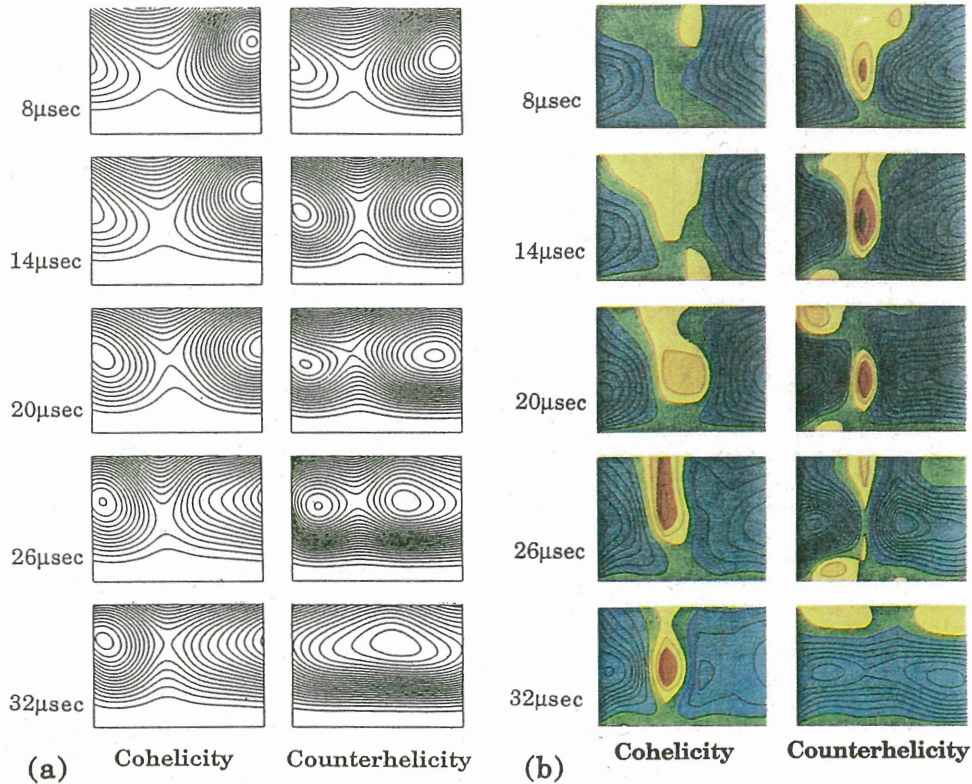


Fig. 3. Time evolution of poloidal flux contours (a) and  $j_t$  contours (b) on the  $r$ - $z$  plane for the cohesivity and counterhelicity mergings.

### 3. Experimental Results

Figure 3(a) shows the time evolutions of 2-D poloidal flux contours for the cohesivity and counterhelicity mergings. In the counterhelicity merging, two magnetic axes merge completely at  $t = 32\mu\text{sec}$ , while the cohesivity merging toroid still has two axes. This difference is interpreted quantitatively in terms of the common flux ratio  $\alpha_c = 2\Psi_{com}/(\Psi_{peak1} + \Psi_{peak2})$ , where  $\Psi_{com}$ ,  $\Psi_{peak1}$  and  $\Psi_{peak2}$  are the poloidal flux function at the reconnection (X) point and those at the two magnetic axes of the merging toroids. Figure 4(a) shows the time evolutions of  $\alpha_c$  for the two mergings. The curves of  $\alpha_c$  clearly reveal that the magnetic reconnection is about three times faster in the counterhelicity merging than in the cohesivity merging. It indicates the significance of the 3-D effect on the reconnection process.

This difference is attributed to the compressibility of the neutral current sheets with and without the magnetic field component parallel to the X-line. Figure 3(b) shows the  $j_t$  profiles of the two merging toroids, where the polarity of  $j_t$  is positive in the blue region (the same as the  $I_t$  polarities of two spheromaks) and negative in the other colored regions. A negative sheet current consistent with theoretical reconnection models is observed around the reconnection region in both cases. Note that the current sheet of the counterhelicity merging toroid is compressed in much shorter time than that of the cohesivity merging. As shown in Fig. 4(b), the maximum sheet current density  $j_{t,max}$  of the counterhelicity merging toroid increases rapidly up to  $1MA/m^2$  until  $t = 18\mu\text{sec}$ , while  $j_{t,max}$  of the cohesivity merging toroid stays about  $0.25MA/m^2$  and then slowly increases. The higher current density generally tends to increase the plasma resistivity, if the averaged drifting speed of electrons significantly exceeds the ion sound velocity. Figure 4(c) shows the time evolutions of the plasma resistivities  $\eta_0$  at

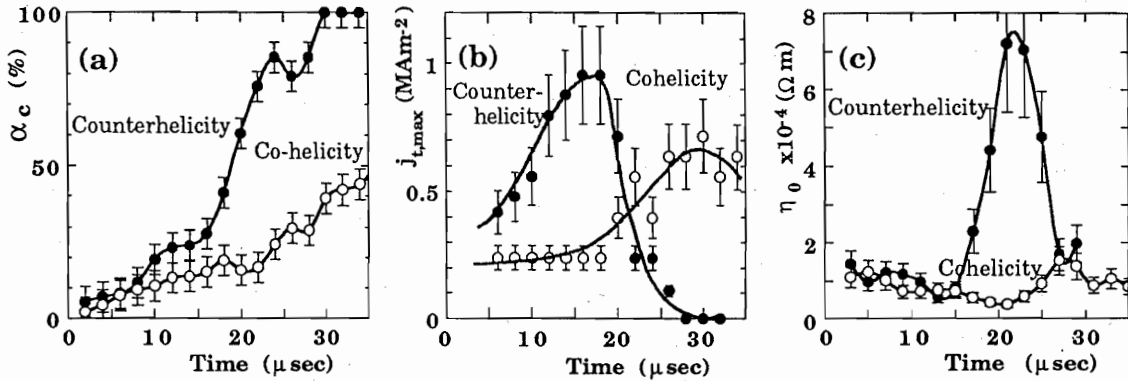


Fig. 4. Time evolution of common flux ratios (a), maximum toroidal current densities  $j_{t,max}$  of the neutral current sheets (b) and plasma resistivities  $\eta_0$  at the X-point (c) for the co-helicity and counterhelicity mergings.

the X-point for the two cases, where  $\eta_0$  is given as the ratio of the toroidal electric field  $E_t = (d\Psi_{com}/dt) / 2\pi r_x$  to  $j_t$  at the X-point. From  $t=5\mu\text{sec}$  to  $15\mu\text{sec}$ , the  $\eta_0$  values of both cases stay about  $5 - 10 \times 10^{-5}\Omega m$ , which is close to the classical Spitzer resistivity  $\sim 5 \times 10^{-5}\Omega m$  calculated from their  $T_e \sim 10eV$  and  $Z=2$  (Helium). However, from  $t=15\mu\text{sec}$  to  $22\mu\text{sec}$ ,  $\eta_0$  of the counterhelicity merging increases up to  $7.2 \times 10^{-4}\Omega m$ , indicating the marked (anomalous) decay of the sheet current. It suggests that the compression of the neutral current sheet is followed by the increase in its anomalous resistivity, resulting in its subsequent faster decay. This is the most probable cause for the faster reconnection of the counterhelicity merging with  $\theta \sim 180^\circ$ . The anomalous resistivity can be due to electrostatic instabilities or magnetic fluctuations. Since a detailed measurement of the fluctuations is yet to be performed, it is difficult to conclude the cause of the observed anomalous resistivity.

Recently, these results are extended by the method (2) to the continuous scan of  $\theta$  from  $\sim 20^\circ$  to  $180^\circ$  as shown in Figs. 1(c) and (c') [2]. The reconnection speed is concluded to increase as  $\theta$  is increased from  $\sim 20^\circ$  to  $180^\circ$ . The reconnection speed also increases proportionally with the initial approaching speed of the two spheromaks [2], suggesting that a compressible driven reconnection model is consistent with our reconnection experiments.

Our experimental results have experimentally revealed a reconnection angle effect on the reconnection speed, which has received increased theoretical attentions by Tajima and Sato [4,5]. This effect is expected to appear not only in laboratory plasmas, for example sawtooth oscillations in Tokamaks with small  $\theta$  and in RFPs with large  $\theta$ , but also in space plasmas, for example the solar corona coalescence [6]. Especially, recent data from the Yohkoh [7] has induced many theoretical considerations on the 3-D magnetic reconnection.

## References

1. Ono, Y. et.al., 1986, *Proc. IEEE Inter. Conf. Plasma Sci., Saskatoon*, 77; Katsurai, M. and Ono, Y., 1987, *Trans. Inst. Electr. Eng. Japan*, 107, 65.
2. Ono, Y. et.al., 1993, *Phys. Fluids B* 5, 3691; Yamada, M. et.al., 1990, *Phys. Rev. Lett.* 65, 721.
3. Ono, Y., et.al., 1993, *Plasma Phys. Cont. Nucl. Fus. Res. 1992, Würzburg* 2, 619.
4. Tajima, T., et.al., 1989, *Fizika Plasmy* 15, 519; Kamimura, T. et.al, 1992, *J. Comp. Phys.* 100, 77.
5. Sato, T., et.al., 1992, *Phys. Fluids B* 4, 450.
6. Sakai J. and Koide S., 1992, *Solar Physics.* 142, 399.
7. Shimizu, T et.al., to be published in *Astrophys. J*; Tsuneta, S., 1991, *Solar Phys.* 136, 37.